J Toxicol Pathol 2012; 25: 273–276

Case Report

Splenic Hemangiosarcoma in a Young Sprague-Dawley Rat

Katsuhisa Shiraki[1*], Mihoko Ono[1], Satoru Kajikawa[1], Ayano Takeuchi[1], Yuichi Murakami[1], Yuji Oishi[1], and Masahiro Matsumoto[1]

[1] Drug Safety Research Laboratories, Astellas Pharma Inc., 1-6 Kashima 2-chome, Yodogawa-ku, Osaka 532-8514, Japan

Abstract: The present report describes a rare case of spontaneous hemangiosarcoma in a nine-week-old male Sprague-Dawley rat. At necropsy, multiple white nodules of various sizes were observed on and within the enlarged spleen and liver and were histopathologically determined to be composed of spindle- to oval-shaped cells that showed invasive growth without encapsulation and were arranged solidly but partially in whorls or faint alveolar patterns with vascular-like spaces containing small clefts or erythrocytes in the tumor mass. Immunohistochemical analysis revealed that most of the tumor cells were strongly positive for vimentin, von Willebrand factor (vWF) and CD34 but negative for podoplanin. In addition, electron microscopic examination revealed the presence of Weibel-Palade bodies in the cytoplasm of the tumor cells. Based on these findings, this case was diagnosed as a hemangiosarcoma. The splenic masses were larger than the hepatic ones, with tumor cells mainly observed at periportal regions with tumor embolism in the liver, suggesting that primary hemangiosarcoma initially developed in the spleen before metastasizing. (DOI: 10.1293/tox.25.273; J Toxicol Pathol 2012; 25: 273–276)

Key words: rat, young, spontaneous, hemangiosarcoma, Weibel-Palade bodies

Spontaneous hemangiomas and hemangiosarcomas may arise in any organs but are often found in the spleen, kidney, subcutaneous tissue and liver in rats[1–3]. The Incidence of hemangiosarcoma in Sprague-Dawley rats ranges from 0.1% to 1.4%, with a mean age at occurrence of 91–104 weeks, and there are no reports among historical control data of occurrence in relatively young animals[4–6]. While hemangiomas are easily distinguished by their tendency to form vascular cavities, histopathological diagnosis of hemangiosarcomas can be difficult without the aid of immunohistochemical techniques, as the tumor's appearance may resemble those of other soft tissue tumors. Here, we describe a case of hemangiosarcoma that occurred spontaneously in a young Sprague-Dawley rat and document the histopathological, immunohistochemical and ultrastructural features of the tumor.

The animal was a nine-week-old male Sprague-Dawley rat Crj:CD (SD) rat purchased from Charles River Laboratories Japan, Inc. (Kanagawa, Japan) for use in a toxicity study. It was housed in a wire mesh cage under controlled conditions (temperature, 23 ± 3°C; relative humidity, 50% ± 20%, 12-h light/dark cycle) and given *ad libitium* access to CRF-1 diet (Oriental Yeast Co., Ltd., Tokyo, Japan) and tap water. The animal was handled in accordance with the Guidelines for Animal Experimentation issued by Astellas Pharma Inc., which are based on the guidelines for animal experimentation issued by the Japanese Association for Laboratory Animal Science. No abnormalities were observed in body weight change, food consumption, clinical signs during the study period or hematology or blood chemistry at the end of treatment, and the animal's final body weight was 374 g. At necropsy, two white masses 12×15×15 mm and 7×7×10 mm in size were observed in the spleen, and multiple small white nodules of varying size (3×3×3 mm at largest) were noted in the liver. The spleen with masses was enlarged, and its absolute and relative weights were 5.8 g and 1.8 g%, respectively, values which deviated substantially from the laboratory's background values (0.55 g and 0.18 g%, respectively). The masses in the spleen were firm in consistency and poorly circumscribed, with multiple red patches on the surface. No abnormalities were noted in any other organs or tissues.

The spleen and liver with the masses, as well as the other organs and tissues, were fixed in phosphate-buffered 10% formalin and then embedded in paraffin and sectioned, at which point they were then subjected to hematoxylin and eosin (H&E) staining for microscopic examination. Sections from the masses were additionally subjected to Masson's trichrome staining and Watanabe's silver impregnation staining. Immunohistochemical examination using the EnVision method was conducted with the antibodies described in Table 1 (EnVision method: staining performed with an EnVision kit [Dako Cytomation, Carpinteria, CA, U.S.A.], detection with EnVision+ [Dako Cytomation], chromogen with 3,3'-diaminobenzidine [Muto Pure Chemicals Co. Ltd., Tokyo, Japan]). For electron microscopic examination,

Received: 28 February 2012, Accepted: 25 June 2012
*Corresponding author: K Shiraki (e-mail: katsuhisa.shiraki@astellas.com)

Table 1. Immunohistochemistry Antibodies

Antibody	Manufacturer	Clone	Antigen source	Monoclonal/ Polyclonal
Vimentin	Dako A/S, Glostrup, Denmark	V9	Porcine eye lens	Mono
Desmin	Dako A/S, Glostrup, Denmark	D33	Human muscle	Mono
Caldesmon	Santa Cruz Biotechnology Inc., CA, U.S.A.	CALD1	Human uterus	Mono
α-Smooth Muscle Actin	Dako A/S, Glostrup, Denmark	1A4	Synthetic α smooth muscle actin	Mono
S100 protein	Dako A/S, Glostrup, Denmark	Code No. Z0311	Bovine brain S100	Poly
Chromogranin A	Dako, CA, U.S.A.	LK2H10	Human chromogranin A	Poly
Cytokeratin	Dako, CA, U.S.A.	Code No. Z0622	Bovine muzzle epidermal keratin subunits of 8, 14 and 18	Poly
CD68	Chemicon International, CA, U.S.A.	ED1	Rat spleen cells	Mono
CD163	Serotec Inc., Oxford, UK	ED2	Rat spleen cells	Mono
CD34	Santa Cruz Biotechnology Inc., CA, U.S.A.	Code No. sc-9095	Human CD34 amino acids 151-290	Poly
Von Willebrand Factor	Dako A/S, Glostrup, Denmark	A0082	Human plasma	Poly
Podoplanin	Sigma-Aldrich Inc., St. Louis, MO, U.S.A.	HG-19	Rat kidney glomeruli and lung	Poly
PCNA	Santa Cruz Biotechnology Inc., CA, U.S.A.	PC10	Rat PCNA	Mono

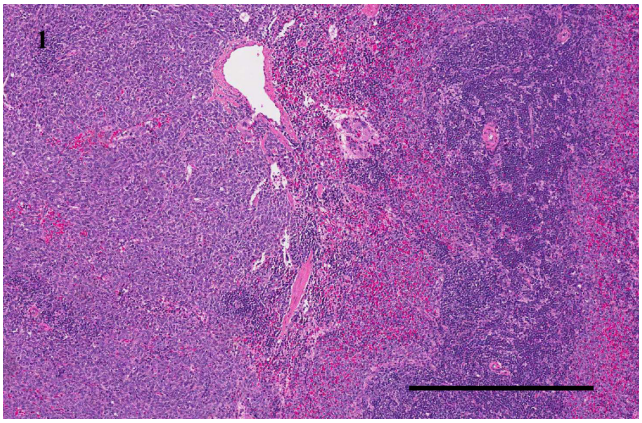

Fig. 1. H&E staining. The tumor replaces most of the normal splenic tissue and is locally invasive without encapsulation (scale bar = 500 µm).

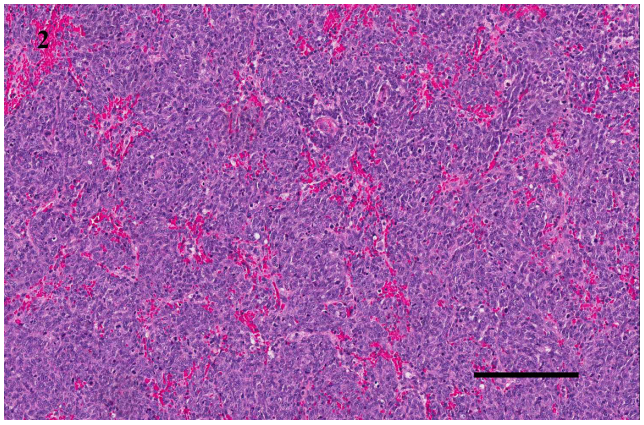

Fig. 2. H&E staining. The mass contains spindle- to oval-shaped cells with scanty stroma and an abortive effort to form vascular structures (scale bar = 200 µm).

pieces of the formalin-fixed mass obtained from the spleen were immersed in phosphate-buffered 2.5% glutaraldehyde and 2% paraformaldehyde for 1 day and then in 1% osmium tetraoxide for 1 h. The tissue samples were embedded in epoxy resin, and ultrathin sections were mounted on Cu/Rh grids, stained with uranyl acetate and lead citrate and observed under a transmission electron microscope (H-600; Hitachi High-Technologies Corp., Tokyo, Japan).

Histopathologically, the tumors replaced most of the normal splenic tissue and were locally invasive without encapsulation. The masses in the spleen were composed of spindle- to oval-shaped cells with basophilic cytoplasm and large, atypical nuclei showing pleomorphism with prominent nucleoli and many mitosis figures (Fig.1 and Fig. 2). While the tumor masses consisted primarily of solid areas with portions showing whorls or faint alveolar patterns, the structure of the tumor cells resembled vascular spaces containing erythrocytes. Thin and brunched reticular fibers were seen around vascular spaces within the tumor, occasionally surrounding tumor cells forming cords and bundles as observed on Masson's trichrome staining and Watanabe's silver impregnation staining (Fig. 3). The tumor cells in the liver showed histological patterns similar to those in the spleen and were primarily located near the periportal spaces, although some had infiltrated into the adjacent parenchyma, leading to loss of hepatocytes. Venous tumor embolisms were occasionally seen in the hepatic veins and the sinusoids. Metastases were found in the sinusoids of the

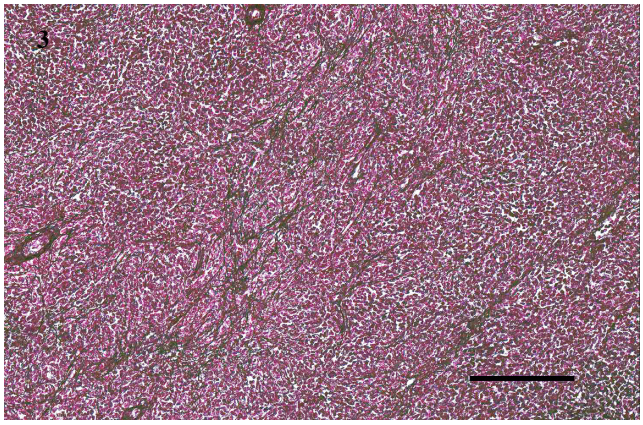

Fig. 3. Watanabe's silver impregnation staining of the mass. Thin and branched reticular fibers can be observed around vascular spaces as well as around tumor cells arranged in cords and bundles (scale bar = 200 μm).

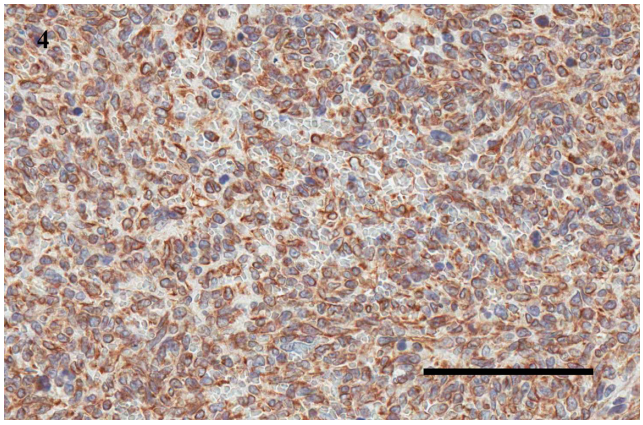

Fig. 4. Immunohistochemistry for vimentin. Tumor cells with atypia are positive for vimentin in the area where neoplastic cells show frequent mitosis and pleomorphism (scale bar = 100 μm).

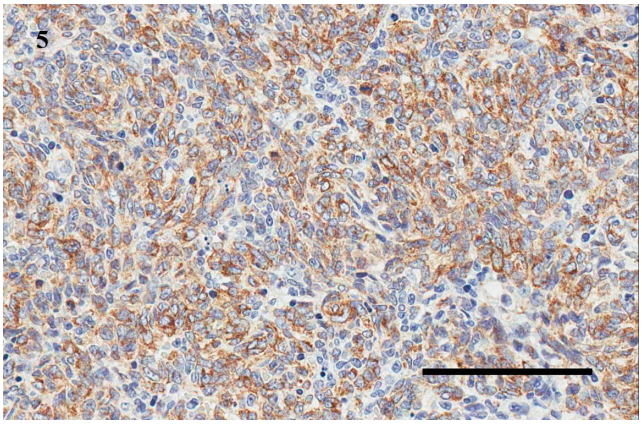

Fig. 5. Immunohistochemistry for vWF. vWF is identified granularly in the cytoplasm of tumor cells (scale bar = 100 μm).

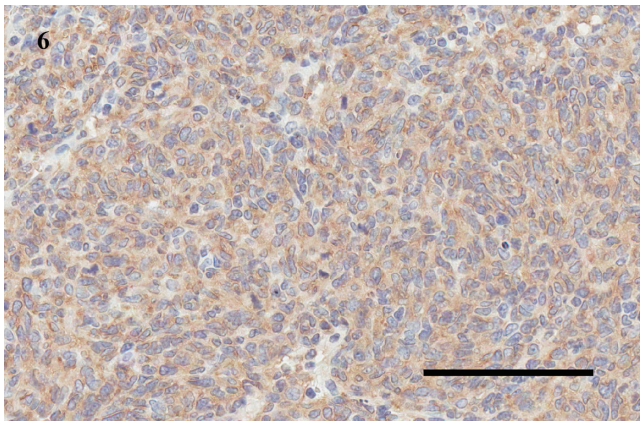

Fig. 6. Immunohistochemistry for CD34. CD34 is identified granularly in the cytoplasm of tumor cells (scale bar = 100 μm).

adrenal medulla and the pancreatic lymph node.

Most of the tumor cells were strongly positive for vimentin (Fig. 4) and negative for cytokeratin. vWF and CD34, both vascular endothelial markers, were identified granularly in tumor cells not only in vascular structures but also in the solid components (Fig. 5 and Fig. 6), while podoplanin, a lymphatic endothelial marker, was not detected in the cells at all. Further, the tumor cells were negative for antibodies against desmin, caldesmon, α-smooth muscle actin, S-100, chromogranin A and CD68/CD163, allowing us to rule out the presence of other soft tissue tumors. The tumor cells also showed a high PCNA labeling index.

Electron microscopic examination showed that the tumor cells contained small populations of mitochondria, a rough endoplasmic reticulum, and tight junctions with neighboring cells. The nuclei were oval to slightly irregular in shape, with prominent peripheral heterochromatin, and several cells contained inconspicuous nucleoli. Weibel-Palade bodies characterized by a single membrane and dense interior with rod-shaped profiles were also occasionally detected. The Weibel-Palade bodies were aligned parallel to the edge of the cells and showed longitudinal striation (Fig. 7).

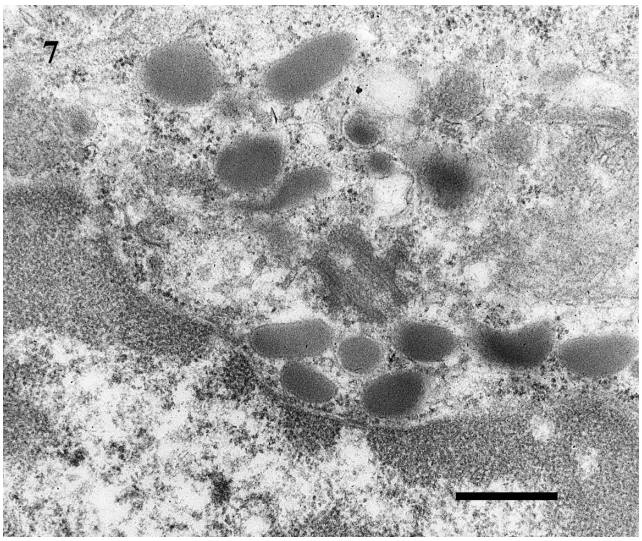

Fig. 7. Electron microscopy of the mass. Weibel-Palade bodies, characterized by a single membrane and dense interior with rod-shaped profiles, can be found in the cytoplasm of tumor cells (scale bar = 500 nm).

The present case involved a soft tissue tumor in which the cell of origin was difficult to determine by routine histopathological examination, as the tumor consisted of a dense sheet of pleomorphic cells frequently observed in undifferentiated tumors. Use of antibodies specific for endothelium cells, such as vWF and CD34, and positive results for vimentin indicated the tumor to be of endothelial origin but did not allow for differentiation between hemangiosarcoma and lymphangiosarcoma, as both tumors express these endothelial markers and show similar histopathologic characteristics. Podoplanin is a specific marker for the lymphatic endothelium that can be used to distinguish lymphangiosarcoma from hemangiosarcoma[7]; given that the tumor was immunohistochemically negative for podoplanin, we were able to rule out lymphangiosarcoma. The presence of Weibel-Palade bodies on electron microscopy further supported our diagnosis of hemangiosarcoma[8, 9], as these structures are typically found in large numbers in arteriolar endothelial cells and are generally believed to be absent in lymphatics[10].

Hemangiosarcomas in rats may occur in the spleen, kidney, subcutaneous tissue and liver, but are found most frequently in the spleen[1–4], often subsequently metastasizing to other abdominal organs[11]. In the present case, the splenic masses were larger than the hepatic ones, with tumor cells mainly observed at periportal regions with tumor embolism in the liver, suggesting that primary hemangiosarcoma initially developed in the spleen before metastasizing.

Several previous two-year-long oncogenicity or lifespan studies in Sprague-Dawley rats have reported that spontaneous hemangiosarcoma occurred in 5 of 1420 animals (incidence rate: 0.4%)[4], 1 of 70 animals (1.4%)[5] and 1 of 880 animals (0.1%)[6], with no clear sex differences in tumor incidence reported. Spontaneous hemangiosarcomas are typically observed in rats aged more than 91 weeks[4], with one study observing the tumor in younger animals following induction by Polyomavirus injection into the central nervous system of Wistar/Furth rats during the neonatal period, leading to hemangiosarcoma development from 14 to 29 days after birth (incidence: 100%)[12]. However, the spontaneous hemangiosarcoma discussed in the present report was found in a 9-week-old rat, a much younger age than that noted in previous reports. Therefore, we felt the need to report this rare case of hemangiosarcoma occurring spontaneously in a young SD rat.

Acknowledgment: We wish to thank Messrs. Kenji Nakano, Shuuji Ishikawa and Takashi Shishido and Ms. Yukiko Nakagawa for their excellent technical assistance.

References

1. Goodman DG, Ward JM, Squire RA, Chu KC, and Linhart MS. Neoplastic and nonneoplastic lesions in aging F344 rats. Toxicol Appl Pharmacol. **48**: 237–248. 1979. [Medline] [CrossRef]
2. Haseman JK, Arnold J, and Eustis SL. Tumor incidences in Fischer 344 rats: NTP historical data. In: Pathology of the Fischer Rat. Reference and Atlas. GA Boorman, SL Eustis, MR Elwell, CA Montgomery Jr, and WF MacKenzie (eds). Academic Press, San Diego. 555-564. 1990.
3. Haseman JK, Hailey JR, and Morris RW. Spontaneous neoplasm incidences in Fischer 344 rats and B6C3F, mice in two-year carcinogenicity studies: a National Toxicology Program update. Toxicol Pathol. **26**: 428–441. 1998. [Medline] [CrossRef]
4. Zwicker GM, Eyster RC, Sells DM, and Gass JH. Spontaneous vascular neoplasms in aged Sprague-Dawley rats. Toxicol Pathol. **23**: 518–526. 1995. [Medline] [CrossRef]
5. Anver MR, Cohen BJ, Lattuada CP, and Foster SJ. Age-associated lesions in barrier-reared male Sprague-Dawley rats: a comparison between Hap:(SD) and Crl:COBS®(CD)®(SD) stocks. Exp Agin Res. **8**: 3–24. 1982. [CrossRef]
6. Lang PL. Spontaneous neoplastic lesions and selected non-neoplastic lesions in the Crl:CD Br rat, from Charles River Laboratories website: http://www.criver.com/sitecollection-documents/rm_rm_r_lesions_selected_non-neo_crlcdbr_rat.pdf.
7. Breiteneder-Geleff S, Soleiman A, Kowalski H, Horvat R, Amann G, Kriehuber E, Diem K, Weninger W, Tschachler E, Alitalo K, and Kerjaschki D. Angiosarcomas express mixed endothelial phenotypes of blood and lymphatic capillaries: Podoplanin as a specific marker for lymphatic endothelium. Am J Pathol. **154**: 385–394. 1999. [Medline]
8. Carstens HB, and Schrodt GR. Ultrastructure of sclerosing hemangioma. Am J Pathol. **77**: 377–386. 1974. [Medline]
9. Ho K-L. Ultrastructure of cerebellar capillary hemangioblastoma. 1. Weibel-Palade bodies and stromal cell histogenesis. J Neuropathol Exp Neurol. **43**: 592–608. 1984. [Medline] [CrossRef]
10. Higgins JC, and Eady RAJ. Human dermal microvasculature: its segmental differentiation, light and electron microscopic study. Br J Dermatol. **104**: 117–129. 1981. [Medline] [CrossRef]
11. Guzman RE, Ehrhart EJ, Wasson K, and Andrews JJ. Primary hepatic hemangiosarcoma with pulmonary metastasis in a New Zealand White rabbit. J Vet Diagn Invest. **12**: 284–286. 2000. [Medline] [CrossRef]
12. Flocks JS, Wells TP, Kleinman DC, and Kirsten WH. Dose-response studies to polyoma virus in rats. J Natl Cancer Inst. **35**: 259–284. 1965. [Medline]